

The γ Velorum binary system

I. O star parameters and light ratio

Orsola De Marco and W. Schmutz

Institut für Astronomie, ETH-Zentrum, Scheuchzerstrasse 7, CH-8092 Zürich, Switzerland

Received 27 August 1998 / Accepted 9 February 1999

Abstract. In this paper we demonstrate how previous determinations of the light ratio between the O and Wolf-Rayet stellar components of the γ Vel system are affected by large uncertainties. This is due, amongst other things, to the difficulty of measuring the equivalent widths of emission and absorption lines. We then present a new technique to de-blend and measure spectral lines, in which we compensate for the observed absorption features with synthetic profiles. From the new values of the diagnostic line strengths we determine a hotter spectral type for the O star companion (O7.5) than previously published.

The light ratio is then determined, together with the stellar parameters, via a spectroscopic analysis. We obtain $\Delta M_V = 1.47 \pm 0.13$ mag. From the light ratio and the system's luminosity we find $M_V(\text{O}) = -5.14$ mag and $M_V(\text{WR}) = -3.67$ mag. Simultaneously we determine $T_{\text{eff}}(\text{O}) = 35\,000$ K, $L(\text{O}) = 2.1 \times 10^5 L_\odot$ and $\mathcal{M}(\text{O}) = 30 M_\odot$. An age of 3.59×10^6 yr is derived from these parameters and evolutionary tracks. We find that the H/He abundance ratio is solar. From a hydrodynamical calculation of the radiation-driven wind we obtain $\dot{M}(\text{O}) = 1.8 \times 10^{-7} M_\odot \text{ yr}^{-1}$ and $v_\infty(\text{O}) = 2500 \text{ km s}^{-1}$.

From the O star mass derived here and the mass ratio from the literature we derive the mass of the Wolf-Rayet star, $\mathcal{M}(\text{WR}) = 9 M_\odot$. The mass-luminosity relation for Wolf-Rayet stars then leads to $L(\text{WR}) = 1.5 \times 10^5 L_\odot$. We finally present the γ Vel Wolf-Rayet spectrum de-convolved from the O star in the range 3800–6700 Å.

Key words: stars: binaries: spectroscopic – stars: early-type – stars: fundamental parameters – stars: individual: γ Vel – stars: Wolf-Rayet

1. Introduction

γ Vel (WR11) was first reported to be a double-lined spectroscopic binary system by Sahade (1955). Smith (1968) determined the spectral class of the Wolf-Rayet (WR) component to be WC8, while the O star component was attributed a variety of spectral classes: O6 (Smith 1955), O7.5 (Ganesh & Bappu 1967), O8 (Baschek & Scholz 1971), O9I (Conti & Smith 1972) and finally O8III (Schaerer et al. 1997).

Due to its binary nature, γ Vel is one of the few systems for which we can directly determine the masses of the O and the WR stars. Schaerer et al. (1997) derived the system's mass, $\mathcal{M}(\text{O+WR}) = 29.5 \pm 15.9 M_\odot$, and absolute visual magnitude, $M_V(\text{O+WR}) = -5.39$, from the HIPPARCOS distance to the γ Vel system, the angular size of the semi-major axis as measured from intensity interferometry, and the orbital period. They determined the stellar effective temperature of the O and WR stars by using non-LTE model atmosphere codes to fit the He I $\lambda 4471$ /He II $\lambda 4541$ line strength ratio, with assumed solar abundance and mass loss rate ($5 \times 10^{-7} M_\odot \text{ yr}^{-1}$). Subsequently Schmutz et al. (1997) re-determined the system's orbital parameters and the mass of the WR component from new radial velocity curves.

St-Louis et al. (1993) interpreted the γ Vel UV spectral variability as arising from eclipsing effects and the presence of a wind-wind collision zone. From their considerations on line variability, they derived the terminal velocities of the O and WR stellar winds to be $v_\infty(\text{O}) = 2330 \text{ km s}^{-1}$ and $v_\infty(\text{WR}) = 1550 \text{ km s}^{-1}$.

The values of the individual luminosities of the two components of the γ Vel system, rest crucially on the determination of the light ratio. This was determined by Conti & Smith (1972) to be $f_V(\text{O})/f_V(\text{WR}) = 3.63 \pm 0.33$, by comparing the equivalent widths of the optical emission lines of the WR star with the equivalent widths of another WC8 star (WR135). This method is based on the claim that equivalent widths of certain emission lines do not change with spectral subtype. Using similar techniques, Willis & Wilson (1976) measured UV emission lines in their spectrophotometry (TD-1A - S2/68) of γ Vel and WR135 to derive a UV brightness difference of $f_V(\text{O})/f_V(\text{WR}) = 5.3 \pm 1.5$, while from continuum measurements they derived $f_V(\text{O})/f_V(\text{WR}) = 3.6$. Stickland & Lloyd (1990) later confirmed these UV-based conclusions from IUE spectra of γ Vel and comparison O stars. The most recent investigation of the light ratio was by Brownsberger & Conti (1993). They applied the same method as Conti & Smith (1972) on spectra obtained with modern linear detectors deriving $f_V(\text{O})/f_V(\text{WR}) = 5.49^{+3.71}_{-2.14}$.

The huge uncertainty in the light ratio, together with the fact that the analysis of Schaerer et al. (1997) only determined the O star temperature with assumed abundance, mass-loss and

wind structure and making use of no line fits, called for a detailed examination of the O star. In this paper we present a full spectroscopic analysis of the O star, to determine its parameters simultaneously with the light ratio through a new fitting technique. Additionally, we de-convolved the γ Vel spectrum from the O star component allowing the WR emission lines to be measured with greater certainty. In a following paper (De Marco et al. in preparation) we will determine the stellar parameters of the WR star using a clumped, line-blanketed stellar atmosphere, and compare the spectroscopic luminosity to that derived from the mass-luminosity relation (Schaerer & Maeder 1992) to attempt the calculation of a WR hydrodynamical wind structure.

In Sect. 2 we describe the observations and data reduction. In Sect. 3 we summarize previous attempts at measuring the light ratio and the uncertainties involved. We then proceed (Sect. 4) to measure the strength of the absorption lines in the spectrum of γ Vel through a new fitting technique. We finally (Sect. 5) determine the light ratio of the O to the WR stellar components together with the stellar parameters of the O star, by using an analysis with hydrodynamic model atmospheres. In Sect. 6 we present our conclusions and the O star-corrected γ Vel spectrum.

2. Observations

Our observations of γ Vel are the same as those used by Schmutz et al. (1997), where a full account of the data reduction can be found. The observational database consists of 133 spectra in the blue wavelength region (3500–5400 Å) and 154 in the red region (5800–8600 Å) covering the binary period, taken at the 50 cm ESO telescope in conjunction with the Heidelberg Extended Range Optical Spectrograph (HEROS). The resolution is $R=20\,000$, while the S/N ratio ranges between 100 at 3600 Å and 250 at 6000 Å.

We obtained a phase-averaged mean spectrum by shifting each spectrum according to the WR radial velocity curve (Schmutz et al. 1997) and taking an average. As a result, the O star absorption features in the mean spectrum appear broadened by the combined orbital Doppler shifts of the O and WR stars. We normalized the mean spectrum by fitting the continuum of the B2 IV star 28 CMa and using the resulting curve to obtain a relative flux calibration; γ Vel could then be rectified using a smooth curve through selected continuum points. This method leads to acceptable results longward of the “Balmer jump”.

3. Former measurements of the O/WR light ratio

In what follows we demonstrate that the light ratio obtained from the WR emission line equivalent widths (EWs) method is subject to large errors due to the emission line EW scatter for stars of equal spectral subtype. We will then show that the same procedure carried out on the O star absorption features is also unreliable, mainly due to the impossibility of measuring accurate EWs for the O star lines.

The light ratio between the WR and O star components of the γ Vel system was measured by Conti & Smith (1972) and by

Table 1. Equivalent width measurements (in Å) for different line blends in five WR stars, compared with the measurements of Conti & Smith (1972). The line blends marked with ‘(:)’ were not used by Conti and Smith in the comparison. The spectral type is according to van der Hucht et al. (1981). For WR77 the errors are gauged at 50%.

Star	Spect. Type	Band Center (Å)			
		3888(:)	4072	4329	4473(:)
This work					
WR60	WC8	13±10	40±10	24±5	1±1
WR135	WC8	24±3	40±8	35±3	10±1
WR57	WC7	13±3	58±5	45±7	2.3±2.0
WR53	WC8	23±3	65±5	41±4	6±3
WR77	WC8.5	0.1	0.7	9	1.4
Conti & Smith (1972)					
WR103	WC9	24	44	32	12
WR135	WC8	22.6	44.6	38.0	11.2

Brownsberger & Conti (1993) by comparing the γ Vel WR star emission line EWs with those of single WC stars. Conti & Smith (1972) investigated the sensitivity of emission line EWs to spectral subtype by comparing the the EWs of WR135 to those of the WC9 star WR103. They selected four temperature-insensitive lines (later excluding two of them due to measurement uncertainty) from which the γ Vel light ratio was determined.

In Table 1 we list our own EW measurements of the same four blends for five WC8 stars from the list of Smith et al. (1990; the spectra from Torres & Massey (1988) are shown in Fig. 1). Excluding WR77, which displays systematically weaker lines (it might well be a binary, given the absorptions at the wavelength of the Balmer lines), and taking into account the individual measurement uncertainties, it is apparent that the EW can vary up to about a factor of two between different stars.

Brownsberger & Conti (1993) analysed 50 spectral lines in a sample of 45 WC stellar spectra obtained with modern linear detectors. Their light ratio value of $f_V(\text{O})/f_V(\text{WR})=5.49$, admits to a 50% uncertainty following the large spread of EW values. The revised ratio is of interest not because of the new value, but because it admits to a much larger uncertainty intrinsic to the method. It must be stressed that such a large uncertainty cannot be tolerated as it implies a large error on the WR stellar luminosity. This method is therefore not useful in constraining the light ratio value to a satisfactory accuracy.

In an analogous way to the WR emission line method, Conti & Smith (1972) compared the O star $\lambda 4471$ EW to the average EW value of a group of O stars of similar spectral subclass. They determined $f_V(\text{O})/f_V(\text{WR})=1.82_{-0.76}^{+2.55}$. The discrepancy with the value obtained from the WR line method was dismissed by Conti and Smith as being consistent with the large errors on the value obtained from the O star EW, and the light ratio from the WR star comparison was therefore adopted.

Aside from the natural scatter of O star line EW values, for stars of equal spectral subtype, the spectral features of the O star component of γ Vel are always blended with emission lines from the WR star. To deconvolve even the simplest WR-O line

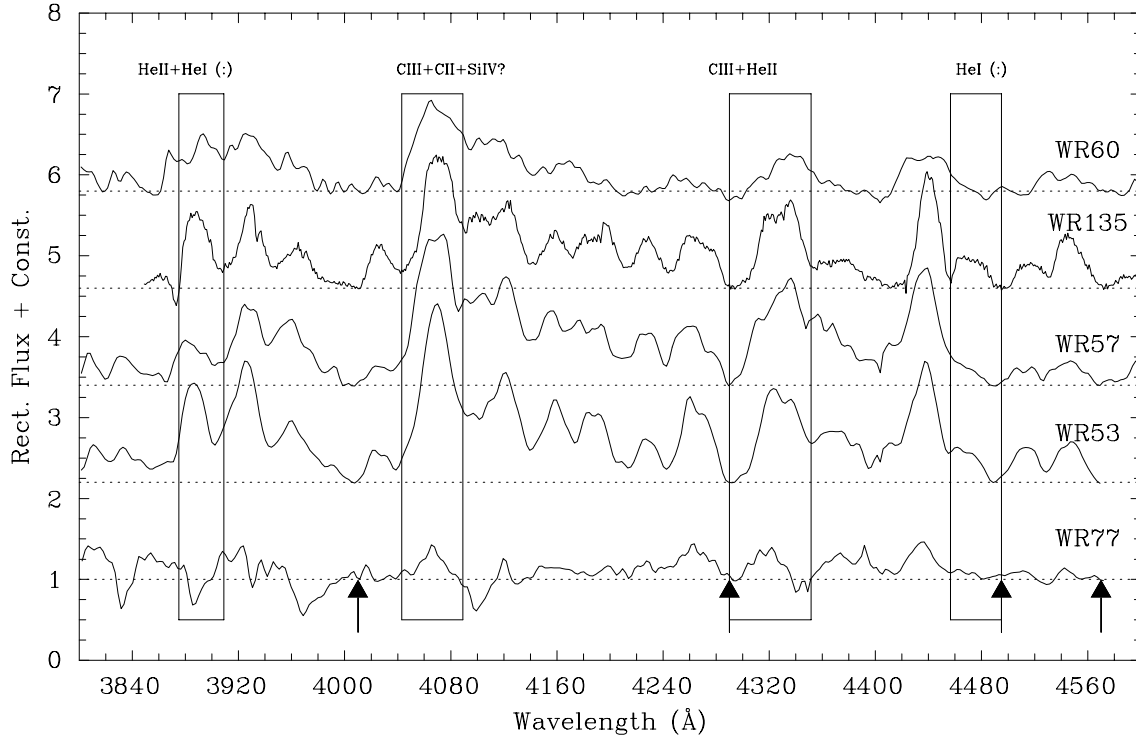


Fig. 1. Comparison of five rectified WC8 (Smith et al. 1990) star spectra. Boxed are the four spectral bands used by Conti & Smith (1972) to determine the light ratio of the O to the WR stellar components of the γ Vel system (the boundaries of the bands were slightly adjusted when carrying out measurements to accommodate for different line widths). The lines identified by Conti & Smith (1972) as being the main contributors to the flux in these bands are labeled. The arrows point to the continuum points selected by Conti & Smith (1972) and used in the rectification. The ‘(:)’ symbol marks the bands not used by Conti and Smith because of uncertain measurements in the γ Vel spectrum.

blends (e.g. the O star $H\beta$ absorption and the WR He II $\lambda 4859$ emission line blend), a double Gaussian deconvolution method is not sufficient: not only are WR stellar line shapes significantly different from Gaussians, but the strong O star absorption lines have extended wings which are completely lost in the blend.

This effect can be appreciated by noticing that the EWs of O star lines measured with a double Gaussian method are phase dependent¹, with the maximum underestimation of the absorption line wings at a phase where the O and WR lines are at the same wavelength.

4. Measurement of the O star line equivalent widths

In Sect. 3 we have discussed the difficulties connected with measuring of the absorption line strengths in the spectrum of γ Vel. We therefore developed a different measurement technique. We derived the O star absorption line EWs by subtracting scaled O star model profiles (see below) from the mean observed spectrum of γ Vel.

To guide the eye we compared the resulting spectrum to that of the WC8 star WR 135², which presents an overall very

¹ This variability can be shown not to be physical in nature, since different absorption lines display different phase dependences.

² An intermediate resolution ($R \sim 2000$) spectrum of WR135 was kindly made available by P.A. Crowther (for details of the acquisition and data reduction procedures see Crowther et al. 1995).

similar spectral morphology to that of γ Vel. We would like to stress that we did not try to reproduce the spectrum of WR135, we only used it to decide on the expected shape of the profiles, i.e. rounded versus flat-topped.

The O star lines in the mean spectrum are broadened by the combined radial velocity shifts of the O and WR stars (cf. Sect. 2). To compare synthetic spectra with the observations, we therefore artificially broadened the synthetic lines by the same amount, using the radial velocity curve (Schmutz et al. 1997) and averaging 133 wavelength-shifted synthetic spectra corresponding to the dates of the observations. The synthetic spectra were also convolved to account for rotational broadening corresponding to a velocity of 220 km s^{-1} (Baade et al. 1990).

The scaling factor for a given model spectrum was chosen by visually determining when the O star features were nulled in the observed spectrum. In Fig. 2 we show O star model spectra in the ranges $4430\text{--}4570 \text{ \AA}$ and $4820\text{--}4950 \text{ \AA}$, multiplied by a range of factors ($f = 0.3, 0.5, 0.6, 0.7, 0.8, 0.9$ and 1.0) and subtracted from the mean spectrum of γ Vel. The vertical lines drawn in each panel of Fig. 2 mark the positions of the features of interest and help the eye to focus attention on the troughs of the O star lines, which are the features to be nulled. To determine which factor nulls the absorption feature, we followed the vertical line from bottom to top to determine for which value of f the trough has disappeared.

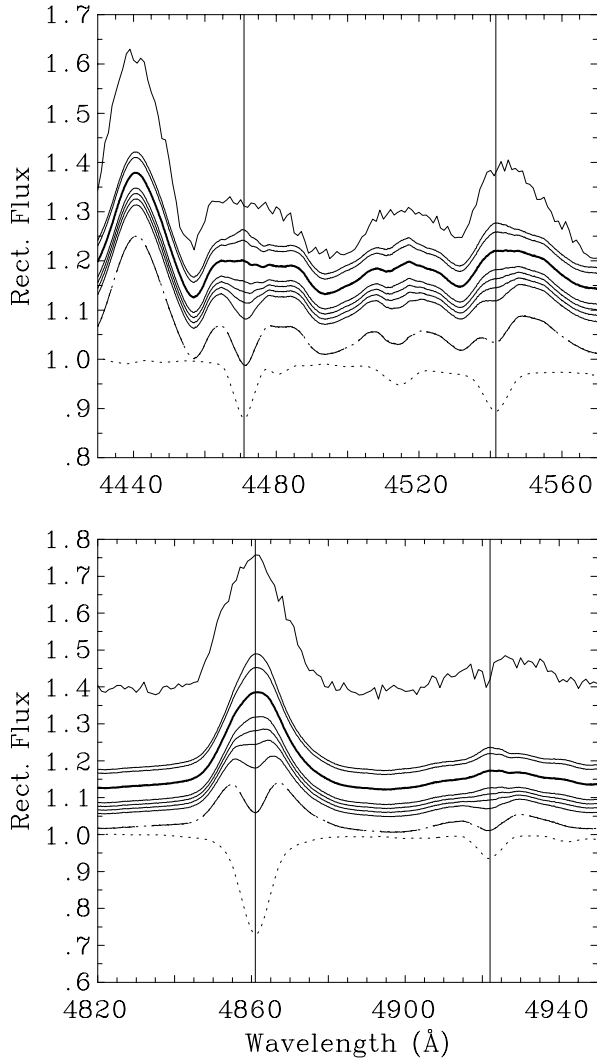


Fig. 2. Example fits to the mean spectrum of γ Vel in the ranges 4430–4570 Å and 4820–4950 Å. From bottom to top of each panel we present the O star model (dotted line), the observations (dot-dashed line), the fits with factors 0.3, 0.5, 0.6, 0.7, 0.8, 0.9 and 1 (where the fit obtained with factor 0.8 is represented by a thicker line), and finally the spectrum of WR135. The model has $T_{\text{eff}}=35\,000$, $\log(\dot{M})=-6.75$ and He/H=0.1.

This procedure was repeated, for every line, using model lines from eight models with different parameters. At this stage we are not using the models described in Sect. 5; we are using those of an O star model grid presented by Schmutz (1998), calculated in the temperature range 30 000–40 000 K with mass-loss ranging between $\log(\dot{M})=-6.5$ and -6.1 , and helium abundance and gravity in the ranges $N[\text{He}]=0.06-0.15$ and $\log(g)=3.5-4.0$. Different models produce lines with different strengths and shapes. While the factor f scales the lines strength, the different line shapes add to the measurement scatter. In this way it was possible to determine a statistical error for the line strengths.

The lines selected for fitting were chosen according to a number of criteria. First, we insured that both upper and lower

Table 2. Equivalent widths (in Å) measured for He I $\lambda\lambda 4471, 4922$ and He II $\lambda 4541$.

Line	Measured EW
He I 4471	0.563 ± 0.010
He II 4541	0.470 ± 0.020
He I 4922	0.320 ± 0.017

transition levels were included in the model atom. Second, we fitted only lines in the same wavelength region for which we had a comparison (WR135; 3840–7300 Å). Third, we excluded particularly crowded regions where the WR spectrum presented complex blends. In Table 2 we list the absorption line EWs of three lines that we have finally selected to carry out the analysis, namely He I $\lambda\lambda 4471, 4922$ and He II $\lambda 4542$. Two other lines were suitable according to the criteria above (H β /He II $\lambda 4859$ and He II $\lambda 4022$) but, due to the underlying WR emission line shapes, it was only possible to determine a lower limit for their strength: this is illustrated in Fig. 2 for the case of H β . As long as the synthetic spectrum is multiplied by factors larger than or equal to 0.7, it compensates for the absorption line, with no clear over-compensation.

In Table 2 we present the determined EW values. These EWs are lower than the values we would measure if the O star were single by a factor equal to the light ratio $f_V(\text{O})/f_V(\text{O}+\text{WR})$. The error estimates listed in Table 2 correspond to the standard error on the mean, σ/\sqrt{N} , where $N=8$ is the number of independent measurements of the line strengths.

The ratio $\log(\text{EW}(\lambda 4471)/\text{EW}(\lambda 4541)) = 0.0792 \pm 0.0181$, implies spectral type O7.5 (where the class boundaries for an O7.5 are 0.0 and 0.10, Mathys (1988)). This is hotter than the estimates of Schaerer et al. (1997; from $\log(\text{EW}(\lambda 4471)/\text{EW}(\lambda 4541)) = 0.204$ they derived O8.5) and Conti & Smith (1972; O9). We understand the difference by considering that the O star He II $\lambda 4541$ line is blended with a round-shaped WR emission line. This means that O star line wings cannot be taken into account by direct measurement or the deconvolution methods, thereby severely underestimating the line strength. On the other hand, the He I $\lambda 4471$ line is blended with a flat-topped WR feature and its wings are partly included when measuring its strength with simple de-blending techniques.

5. Spectroscopic analysis of the O star

If the brightness ratio of the O and WR stars were known, we would at this point multiply the measured EWs by it and proceed in matching the resulting line strength with our non-LTE models. However since the light ratio is not determined, we have to treat it as another unknown of the spectroscopic analysis. Below we describe the procedure we followed to determine the stellar parameters together with the light ratio.

An analysis of the O star spectrum is severely hampered by the fact that many diagnostic lines cannot be measured accurately. This implies that we cannot use the standard procedure

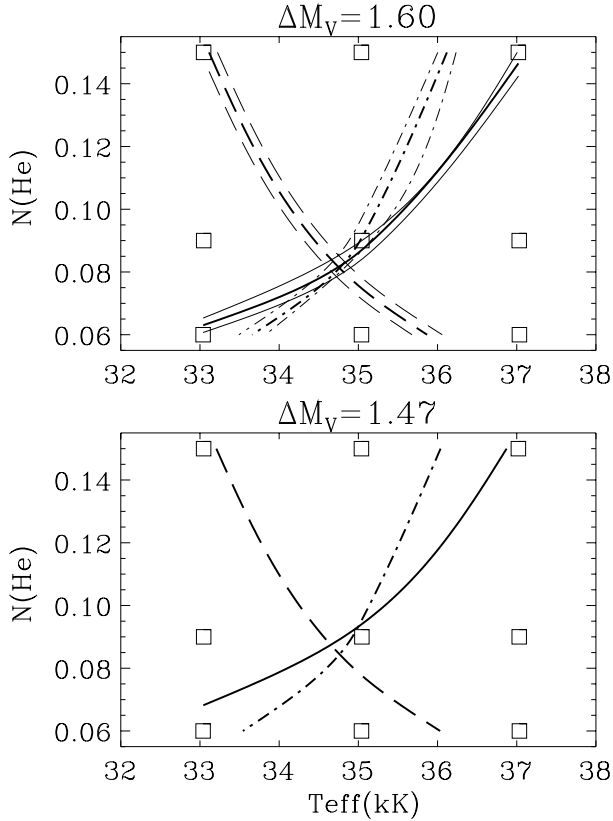


Fig. 3. Equivalent width contours on the helium abundance-temperature plane for the He I $\lambda 4471$ (solid line), He II $\lambda 4541$ (dashed line) and He I $\lambda 4922$ (dot-dash line), for light ratios corresponding to $\Delta M_V = 1.60$ (upper panel) and 1.47 (lower panel). The thin contour lines in the upper panel represent the error estimates (they have been omitted in the lower panel for clarity). Square symbols mark the parameter coordinates for which the models were calculated.

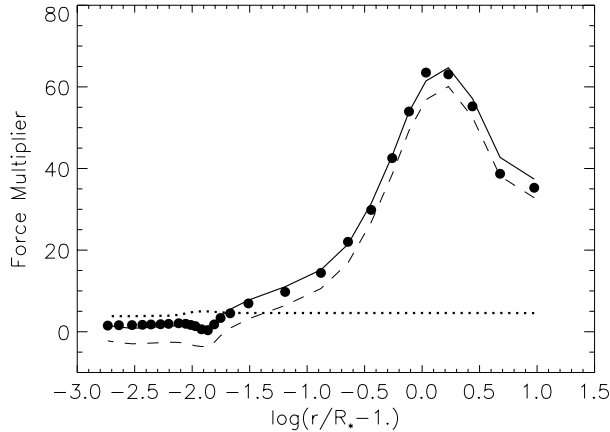


Fig. 4. Comparison of the calculated force multiplier (filled circles) with the factors needed to drive the wind (full-drawn line). The dashed line illustrates the contribution by the kinematic term, i.e. the multiplier required for the acceleration of the wind without inclusion of gravitation, and the dotted line gives the factors needed to support the material against gravity. The unit of the force multiplier is the radiative force on electrons.

to derive parameters of a stellar atmosphere. In particular, there are no line wings of hydrogen Balmer lines that could be used to diagnose the gravity, nor are there any lines that indicate the mass loss rate, such as He II $\lambda 4686$ or H α . These two lines are blended with very strong WR He II features and the measuring procedure outlined in Sect. 4 is unreliable, i.e. we can only derive lower limits for their strengths.

Our approach consists in eliminating as many free parameters as possible by using state-of-the-art hydrodynamic atmospheres. In this way we replace all the parameters related to the density structure, i.e. gravity, velocity law, and mass loss rate, by the stellar mass. This newly introduced parameter is much less problematic because it can be calculated reliably from the stellar luminosity through the mass-luminosity relation given by stellar evolution calculations (Meynet et al. 1994).

We start the analysis by constructing a hydrodynamic atmosphere/wind density structure with the method described in Schaerer & Schmutz (1994) based on the stellar parameters of the O star given by Schaerer et al. (1997). However, in the first part of our analysis, our approach differs from that of Schaerer & Schmutz (1994) in that we do not iterate for consistency between the line force and the calculated structure – this will be done only later for the final model. This means that the density structure at this stage is preliminary. In order to allow a comparison with the final values, we give here the preliminary solution of the critical point equation, which leads to $\dot{M} = 1.3 \times 10^{-7} M_{\odot} \text{ yr}^{-1}$ and the integration of the equation of motion which predicts a terminal velocity of $v_{\infty} = 2700 \text{ km s}^{-1}$. Given these parameters, we then calculated a grid of nine models with $T_{\text{eff}} = 33, 35,$ and 37 kK and with helium abundances $N[\text{He}] = 0.06, 0.09,$ and 0.15 by number.

In Table 2 we have listed the measured strengths of the commonly used temperature diagnostic lines, He I $\lambda 4471$ and He II $\lambda 4541$, and in addition, of He I $\lambda 4922$. In Fig. 3 we display two diagnostic diagrams, corresponding to different brightness ratios ΔM_V . In each diagram we draw contours of constant line strengths in the $T_{\text{eff}}-N[\text{He}]$ plane by interpolation between the nine models. The plotted contours correspond to the inferred line strength values as listed in Table 2, multiplied by $f_V(O + WR)/f_V(O) = 1.23$ and 1.26 , corresponding to $\Delta M_V = 1.60$ and 1.47 , respectively.

As can be seen in Fig. 3, for $\Delta M_V = 1.6$ all three contours meet in one point. This means we have found the stellar parameters and brightness ratio that reproduce the observed line strengths. The precision of this rests in the errors listed in Table 2. These represent the standard error on the mean of eight independent measurements carried out as outlined above. In Fig. 3 (upper panel) the two thin contour lines neighboring each of the main line strength contours, indicate the standard error on the mean observed EWs reduced by $\sqrt{3}$. In this way the area delimited by the intersection of the error contours represents one-standard-deviation for the solution value. We point out, however, that this value takes into account only the line strength uncertainty, but no systematic errors of the atmosphere models.

Within the precision of the measured line strengths, we note that the fit region indicates a solar abundance. We conclude that the helium abundance of the O star is not enriched, i.e.

$$N[\text{He}] = 0.087.$$

We then adjust the ratio ΔM_V such that the center of the fit triangle is located at the chosen abundance, this happens for (Fig. 3-lower panel)

$$\Delta M_V = 1.47^{+0.33}_{-0.13}$$

The error on this estimate is obtained by shifting the value of ΔM_V below and above the chosen value, until three error contours cannot intersect each other at only one point. In this way the error on ΔM_V represents 1 standard deviation. We notice that the lower error bar would shift the fit triangle to an abundance value of $N[\text{He}]=0.076$, which is below the solar value and thus unlikely to be correct.

In principle we can also read from the diagnostic diagram the effective temperature. However, at this stage we iterate for a consistent solution of the equation of motion, the radiative transfer, the non-LTE solutions of the rate equations, and the evaluation of the radiative force (for details see Schaerer & Schmutz 1994). After nine iterations we obtain a satisfactory agreement between the forces calculated for a model that reproduces the observed line brightness and the forces required for the density and velocity law (see Fig. 4). We derive

$$T_{\text{eff}} = 35\,000\text{K}$$

$$R_* = 12.4 R_\odot$$

$$L = 2.1 \times 10^5 L_\odot$$

$$\dot{M} = 1.8 \times 10^{-7} M_\odot \text{yr}^{-1}$$

$$v_\infty = 2500 \text{ km s}^{-1}$$

$$\mathcal{M} = 30 M_\odot.$$

The radius is derived from the brightness of the system, $M_V(\text{sys}) = -5.39$ (Schaerer et al. 1997) and $\Delta M_V = 1.47$, which implies $M_V(\text{O}) = -5.14$, and the predicted astrophysical flux at 5555 \AA of $f_V = 1.72 \times 10^8 \text{ erg cm}^{-2} \text{ s}^{-1} \text{ \AA}^{-1}$. The mass results from the mass-luminosity relation of Meynet et al. (1994). From the grid of evolutionary models we determine, at the place of our parameters in the HR-diagram that $\log L = 3.605 \log \mathcal{M}$. From the isochrones of Meynet et al. (1994; without rotation) and our temperature and luminosity for the O star, we can derive the age of the system to be $(3.59 \pm 0.16) \times 10^6 \text{ yr}$. The small uncertainty (see Fig. 5) takes into account the errors on the luminosity and effective temperature. The uncertainty arising from the neglect of rotation in the calculation of the theoretical tracks may be substantially larger.

In Fig. 6 we illustrate the final model by its electron temperature and velocity as functions of the Rosseland optical depth. The temperature's accuracy is 300 K, from comparing the final model with the effective temperature implied by the fit diagram (Fig. 3). The error on the temperature therefore admits an uncertainty in the density structure. The radius carries an uncertainty of 14% (from the error on the HIPPARCOS distance). The

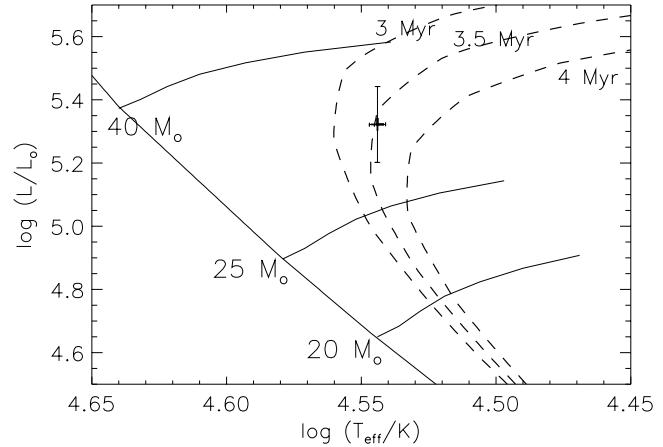


Fig. 5. Luminosity-effective temperature diagram from Meynet et al. (1994). The solid lines are the evolutionary tracks corresponding to 20, 25 and $40 M_\odot$, while the dashed lines are isochrones corresponding to 3, 3.5 and 4 Myr. Our star's position is marked by a cross, which also indicates the size of the uncertainty.

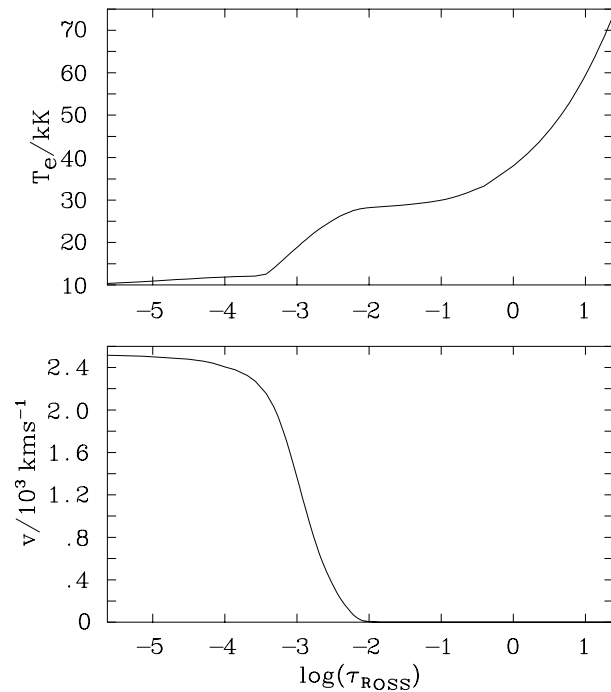


Fig. 6. The run of electron temperature and velocity as functions of the Rosseland optical depth for our final model.

luminosity, on the other hand, inherits an error of about 30%, which leads to an error on the mass of 7%. An independent test of our hydrodynamic star model is possible by comparing v_∞ to the value determined observationally by St. Louis et al. (1993) of 2330 km s^{-1} . In view of systematic deviations of hydrodynamic wind models (Lamers & Leitherer 1993; Puls et al. 1996) and the difficulty to measure the terminal wind velocity for the O star, the agreement is satisfactory. On the other hand, if we adopted $v_\infty^{\text{obs}} = 2330 \text{ km s}^{-1}$ as the correct O star velocity, we can obtain a mass estimate for the O star from the hydrodynamic solution of

the equation of motion. We find that with $\mathcal{M}=27 M_{\odot}$, the solution of the critical point equation yields $\dot{M}=2.2 \times 10^{-7} M_{\odot} \text{ yr}^{-1}$ and terminal wind velocity of 2320 km s^{-1} . This mass is within the uncertainty implied by the error on the luminosity and the systematic uncertainty introduced by neglecting rotation in the evolutionary models (Maeder 1999, Langer 1999). The error on the mass loss and terminal velocity can thus be gauged around 20% and 10%, respectively.

The revised values for the luminosities of the two stars and the other model parameters are summarized in Table 3 along with the results of Schaerer et al. (1997). In Table 3 we also list the EW values for the three measured lines (from Table 2), corrected for the light ratio. Their uncertainties result from those on the measurements and the error on the light ratio. With $\mathcal{M}(\text{O}) \cdot \sin^3 i = 21.6$ from the orbital solution of Schmutz et al. (1997) and our $\mathcal{M}(\text{O}) = 30 M_{\odot}$, we determine a value for the orbital inclination of $i = (63 \pm 8) \text{ deg}$ (St-Louis et al. 1993 derive 70 deg , while Schmutz et al. 1997 find $65 \pm 8 \text{ deg}$). The mass of the WR star is derived from their $\mathcal{M}(\text{WR})/\mathcal{M}(\text{O}) = 0.31$ to be $9.0 M_{\odot}$, from which a luminosity of $1.5 \times 10^5 L_{\odot}$ is implied from the mass-luminosity relation of Schaerer & Maeder (1992).

In Figs. 7 and 8 we present the synthetic O star spectrum, multiplied by $f_V(\text{O})/f_V(\text{O+WR}) = 0.795$ and the spectrum of γ Vel before (dotted line) and after (solid line) subtraction of the O star synthetic spectrum, in the range $3800\text{--}6700 \text{ \AA}$ (we only show the spectral regions where O star lines are present). We also present the spectrum of WR135 reduced by $f_V(\text{O+WR})/f_V(\text{WR}) = 4.87$ so as to compare with the spectrum of γ Vel. As can be observed, the overall morphology of the corrected spectrum follows closely that of WR135. In particular we notice how the WR He II lines corresponding to the Balmer series have recovered their strength. It would have been preferable to measure and analyse more than three lines. On the other hand, all the hydrogen and helium O star lines are very well represented by our model, in that they are compensated for in the combined spectrum (Figs. 7 and 8). The model spectrum also includes metal lines. These are less reliable because LTE populations were used to predict their strengths. This should not interfere with our analysis, since no inherently strong metal lines were present in the spectral regions used to carry out the helium line strength measurements.

6. Discussion

We have calculated a model for the O star of the γ Vel system. Contrary to the analysis of Schaerer et al. (1997) we do not assume a light ratio between the O and WR star components of the γ Vel system, but we determine it along with the other parameters. Our light ratio value of $\Delta M_V = 1.47_{-0.13}^{+0.33} \text{ mag}$ is consistent with that of Conti & Smith (1972) of 1.4 and the more recent value obtained by Brownsberger and Conti (1993) of $1.85 \pm 0.56 \text{ mag}$. We stress that the modern analysis of Brownsberger and Conti uncovers the large uncertainty inherent to the light ratio determined by the WR comparison method and that this uncertainty was not acceptable as most of the system's pa-

Table 3. Summary of the O star parameters. The HIPPARCOS distance of $258_{-31}^{+41} \text{ pc}$ is adopted for the distance-dependent parameters. From it a $M_V(\text{O+WR}) = -5.39 \text{ mag}$ is calculated.

Parameter	This work	Schaerer et al.
$\Delta M[\text{mag}]$	1.47 ± 0.13	1.4
$f_V(\text{O})/f_V(\text{O+WR})$	0.795 ± 0.020	0.78
$M_V(\text{O})[\text{mag}]$	-5.14 ± 0.16	-5.12
$M_V(\text{WR})[\text{mag}]$	-3.67 ± 0.16	-3.86
$T_{\text{eff}}[\text{K}]$	$35\,000 \pm 300$	$34\,000 \pm 1500$
$N[\text{He}][\text{by number}]$	0.087 ^a	–
$R[R_{\odot}]$	12.4 ± 1.7	–
$L(\text{O})[L_{\odot}]$	$(2.1 \pm 0.6) \times 10^5$	$(2.0 \pm 0.7) \times 10^5$
$L(\text{WR})[L_{\odot}]$	$(1.5 \pm 0.5) \times 10^5$	1.1×10^5
$\mathcal{M}(\text{O})[M_{\odot}]$	30 ± 2	29 ± 4
$\mathcal{M}(\text{WR})[M_{\odot}]$	9.0 ± 2.0	7.7 ± 2.5
$\log(\dot{M}/M_{\odot} \text{ yr}^{-1})$	-6.75 ± 0.09	–
$v_{\infty}[\text{km s}^{-1}]$	2500 ± 250	–
$i[\text{deg}]$	63 ± 8	70 ± 10
age(O) [yr]	$(3.59 \pm 0.16) \times 10^6$	–
EW(He I $\lambda 4471$)	0.708 ± 0.030	–
EW(He II $\lambda 4541$)	0.591 ± 0.049	–
EW(He I $\lambda 4922$)	0.403 ± 0.059	–

^a For the uncertainties on this value see the text.

rameters are affected by it. In view of this, we have significantly improved the accuracy of the light ratio of the O and WR star components of the γ Vel system. In addition we note that ratios larger than about $\Delta M_V = 1.6$ require a considerable helium under-abundance, which we consider to be unlikely. We therefore adopt $\Delta M_V = 1.47 \pm 0.13 \text{ mag}$.

We have determined O star parameters, some for the first time (abundance, mass-loss, gravity), while others were revised from the preliminary analysis of Schaerer et al. (1997). It is only due to the combination of two counteracting effects that our parameters turn out to be similar to those of Schaerer et al. (1997). In particular, the smaller He I $\lambda 4471$ /He II $\lambda 4541$ ratio found by us would imply a considerably higher temperature than found by Schaerer et al. (hence the revised spectral type), but this was counterbalanced by a different stellar structure determined by our hydrodynamic calculation. From the weakness of our *synthetic* He II line $\lambda 4686$, we deduce a luminosity class II (Walborn & Fitzpatrick 1990). The other two luminosity criteria, the strengths of S IV and N III lines, cannot be used here, since our model assumes the abundance of metals and, from the purely observational point of view, blending prevents any straightforward conclusion for weak lines. Incidentally, we notice that our derived $M_V(\text{O}) = -5.14 \text{ mag}$ is more in agreement with a luminosity class III/V (Howarth & Prinja 1989).

Most of the O star line strengths have been found to be larger than in previous studies, since the line wings are now accounted for. This is reflected in the revised spectral type, O7.5, that is hotter than the recent determination of Schaerer et al. (1997). The strength of the WR features increases in proportion. In particular “round”-top and “triangular”-shaped WR line strengths are severely affected. For instance the O star H β line EW is 1.37 \AA

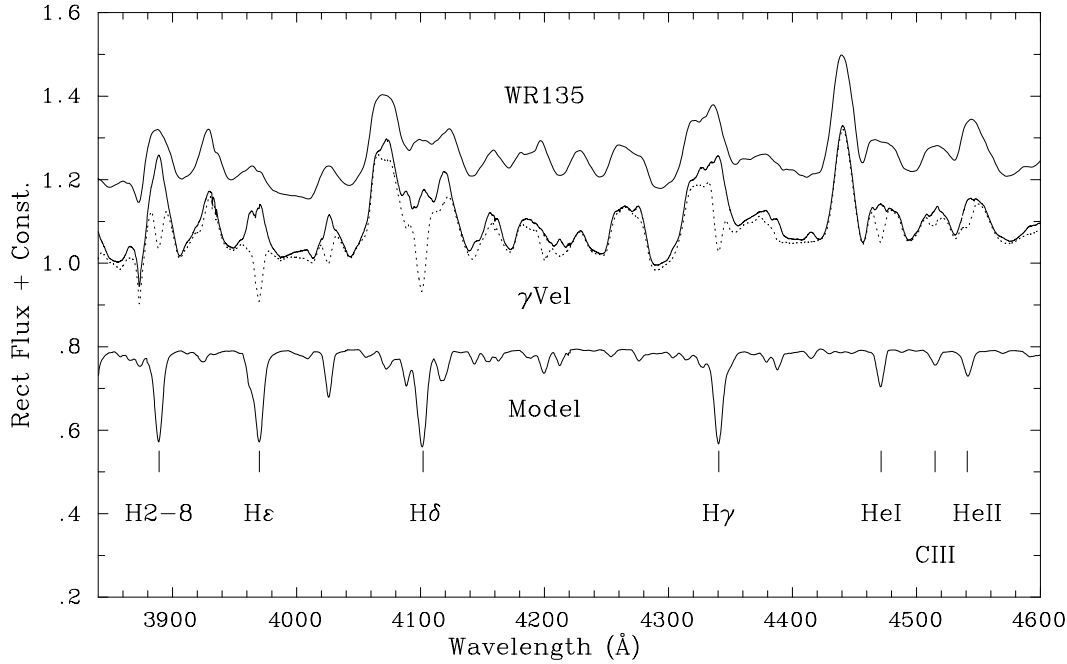


Fig. 7. From bottom to top we present the O star model (in the range 4000–4600 Å – $T_{\text{eff}}=35\,000$ K, $\log(\dot{M}/M_{\odot} \text{ yr}^{-1}) = -6.75$, $\mathcal{M}=30M_{\odot}$ multiplied by $f_V(\text{O})/f_V(\text{O}+\text{WR})=0.795$), the observed spectrum of γ Vel before (dotted line) and after (solid line) subtraction of the scaled O star model, and the scaled spectrum of WR135. The main hydrogen, helium and carbon lines in the O star synthetic spectrum have been labeled.

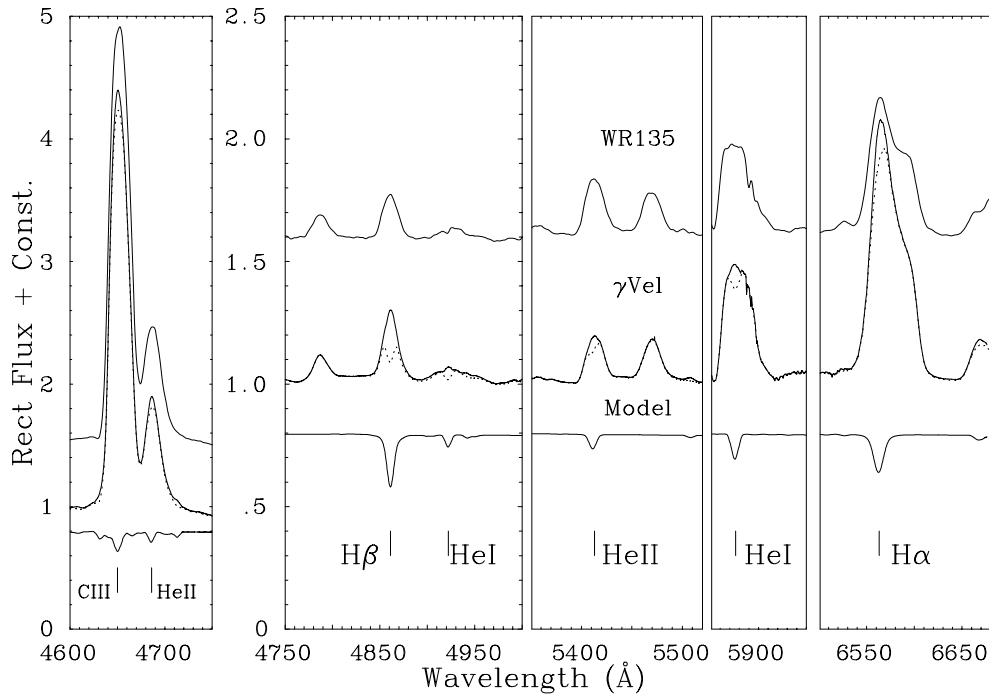


Fig. 8. As in Fig. 7, but for the spectral range 4600–6700 Å – where only regions where O star lines are present have been displayed.

when measured with a double-Gaussian de-blending technique and 2.28 Å when de-blended with our model. Similarly for the WR counterpart, the EW value changes from 4.17 Å to 5.22 Å, which is an increase of 25%.

Finally, we have determined the mass ($\mathcal{M}(\text{WR}) = 9.0 M_{\odot}$) and the luminosity ($L(\text{WR}) = 1.5 \times 10^5 L_{\odot}$) of the WR star,

which will lead to an interesting comparison with the spectroscopic luminosity resulting from our stellar atmosphere analyses (De Marco et al., in preparation).

Acknowledgements. We are thankful to Jörg Schweickhardt who processed the observational material on which this work is based and Paul Crowther for letting us access the spectrum of WR135. We also thank

G. Meynet and N. Langer for educational discussions on the influence of rotation on the evolutionary tracks. Finally, we acknowledge A. Moffat for his comments which improved the focus of this paper.

References

- Baade D., Schmutz W., van Kerkwijk M., 1990, *A&A* 240, 105
 Baschek B., Scholz M., 1971, *A&A* 11, 83
 Brownsberger K.R., Conti P.S., 1993, In: Cassinelli J.P., Churchwell E.B. (eds.) *Massive stars: their Lives in the Interstellar Medium*. ASP Conf. Proc. 35, ASP, San Francisco, 275
 Conti P.S., Smith L.F., 1972, *ApJ* 172, 623
 Crowther P.A., Hillier D.J., Smith L.J., 1995, *A&A* 293, 172
 Ganesh K.S., Bappu M.K.V., 1967, *Kodaikanal Obs. Bull. Ser. A* 183,77
 Howarth I.D., Prinja R.K., 1989, *ApJS* 69, 527
 Lamers H.J.G.L.M., Leitherer C., 1993, *ApJ* 412, 771
 Langer, N., 1999, In: van der Hucht K.A., Keonisberger G., Eenens P.R.J. (eds.) *Wolf-Rayet Phenomena in Massive Stars and Starburst Galaxies*. IAU 193, ASP, in press
 Maeder A., 1999, In: van der Hucht K.A., Keonisberger G., Eenens P.R.J. (eds.) *Wolf-Rayet Phenomena in Massive Stars and Starburst Galaxies*. IAU 193, ASP, in press
 Mathys G., 1988, *A&AS* 76, 427
 Meynet G., Maeder A., Schaller G., Schaerer D., Charbonnel C., 1994, *A&AS* 103, 97
 Puls J., Kudritzki R.P., Herrero A., et al., 1996, *A&A* 305, 171
 Sahade J., 1955, *PASP* 67, 348
 Schaerer D., Maeder A., 1992, *A&A* 263, 129
 Schaerer D., Schmutz W., 1994, *A&A* 288, 231
 Schaerer D., Schmutz W., Grenon M., 1997, *ApJ* 484, L153
 Schmutz W., Schweickhardt J., Stahl O., et al., 1997, *A&A* 328, 219
 Schmutz W., 1998. In: Howarth I.D. (ed.) *Boulder-Munich II: the Properties of Hot, Luminous Stars*. ASP Conf. Proc. 131, ASP, San Francisco, 119
 Smith H.J., 1955, Ph.D. Thesis, Harvard University
 Smith L.F., 1968, *MNRAS* 140, 409
 Smith L.F., Shara M.M., Moffat A.F.J., 1990, *ApJ* 358, 229
 Stickland D.J., Lloyd C., 1990, *Observatory* 110, 1
 St-Louis N., Willis A.J., Stevens I.R., 1993, *ApJ* 415, 298
 Torres-Dodgen A., Massey P., 1988, *AJ* 96, 1076
 van der Hucht K.A., Conti P.S., Lundström I., Stenholm B., 1981, *Space Sci. Rev.* 28, 227
 Walborn N.R., Fitzpatrick E.L., 1990, *PASP* 102, 379
 Willis A.J., Wilson R., 1976, *A&A* 47, 429